MDPI

Article

Effect of Tool Positioning Factors on the Strength of Dissimilar Friction Stir Welded Joints of AA7075-T6 and AA6061-T6

Amir Ghiasvand [1], Saja Mohammed Noori [2], Wanich Suksatan [3], Jacek Tomków [4], Shabbir Memon [5] and Hesamoddin Aghajani Derazkola [6,*]

1 Department of Mechanical Engineering, University of Tabriz, Tabriz 5166616471, Iran; amir.ghiasvand@tabrizu.ac.ir
2 Department of Computer Network, College of Engineering and Computer Science, Lebanese French University, Erbil 44001, Iraq; saja.mohammed@lfu.edu.krd
3 Faculty of Nursing, HRH Princess Chulabhorn College of Medical Science, Chulabhorn Royal Academy, Bangkok 10210, Thailand; wanich.suk@cra.ac.th
4 Institute of Manufacturing and Materials Technology, Faculty of Mechanical Engineering and Ship Technology, Gdańsk University of Technology, Gabriela Narutowicza Street 11/12, 80-233 Gdańsk, Poland; jacek.tomkow@pg.edu.pl
5 Department of Mechanical Engineering, Wichita State University, Wichita, KS 67260-133, USA; sxmemon@shockers.wichita.edu
6 Department of Mechanical Engineering, Islamic Azad University of Nour Branch, Nour 21655432, Iran
* Correspondence: h.aghajany@live.com

Abstract: Friction Stir Welding (FSW) is a solid-state bonding technique. There are many direct and indirect factors affecting the mechanical and microstructural properties of the FSW joints. Tool offset, tilt angle, and plunge depth are determinative tool positioning in the FSW process. Investigating the effect of these factors simultaneously with other parameters such as process speeds (rotational speed and translational speed) and tool geometry leads to a poor understanding of the impact of these factors on the FSW process. Because the three mentioned parameters have the same origin, they should be studied separately from other process parameters. This paper investigates the effects of tilt angle, plunge depth, and tool offset on Ultimate Tensile Stress (UTS) of joints between AA6061-T6 and AA7075-T6. To design the experiments, optimization, and statistical analysis, Response Surface Methodology (RSM) has been used. Experimental tests were carried out to find the maximum achievable UTS of the joint. The optimum values were determined based on the optimization procedure as 0.7 mm of tool offset, 2.7 degrees of tilt angle, and 0.1 mm of plunge depth. These values resulted in a UTS of 281 MPa. Compared to the UTS of base metals, the joint efficiency of the optimized welded sample was nearly 90 percent.

Keywords: friction stir welding; tool offset; tilt angle; plunge depth; ultimate tensile strength

1. Introduction

Friction Stir Welding (FSW) is a relatively new method used for joining similar or dissimilar materials together and classified in solid state joining processes [1,2]. Rotation, penetration, and linear traveling of a non-consumable tool causes material joining [3]. Generated heat by friction between tool and workpiece and materials plastic flow are the main factors of materials joining [4]. Many factors affect mechanical and metallurgical properties of FSW joints, which can be categorized in two main groups: tool geometry and process parameters [5]. Tool geometry parameters are pin and shoulder shapes [6]. Process parameters of FSW include traveling speed, rotational speed, downward force on tool, plunge depth, tilt angle, and tool offset, which have direct effect on materials plastic flow pattern and heat generation and distribution [7]. By varying mentioned parameters, plastic flow and generated heat experience significant changes, which affect microstructures and mechanical properties of joints [8,9]. Three out of six process parameters, namely tilt angle,

plunge depth, and tool offset, are directly in connection with tool position [3,10]. Tilt angle has a great effect on materials forging and moving plastic flow to weld-line [4,11]. The weld nugget and defect density experience significant changes by varying this parameter [12,13]. Plunge depth indicates the tool shoulder penetrating in workpiece, which causes a great amount of friction and plastic flow at the upper part of the workpiece and can lead to extensive changes in the stir zone [14]. Tool offsetting in FSW of dissimilar materials is a way to balance the plastic flow generation and can strongly affect the mechanical and metallurgical properties of joint [15]. By proper adjustment of mentioned parameters, one can achieve a defect-less joint.

There are a few studies on the effect of plunge depth, tilt angle, and tool offset in the FSW process. Kumar et al. [16] investigated the tilt angle effect on mechanical properties of FSW of AISI 316L. Three degrees named 0, 1.5, and 3 were chosen and it was found that at a degree of 1.5, the highest value of UTS could be gained. It was also observed that tilt angle affects the stir zone, maximum temperature, and shear layer under the tool shoulder. Rajendran et al. [17] studied the effects of tilt angle on strength and hardness of joint in FSW of AA2024 Aluminum alloy and recognized that at degrees of 1 to 3, a defect-less joint is achieved. Zheng et al. [18] investigated the effects of plunge depth on mechanical and microstructural properties of FSW of dissimilar 2A70 Aluminum alloy and Inconel 6000 Nickel-base alloy. The range of 0–0.5 mm was chosen for plunge depth. It was found that plunge depth strongly affects the joint strength. In another work, Ramachandran et al. [19] found that the tool offset has a great effect on microstructures and mechanical properties of HSLA steel and AA5052-H13 Aluminum alloy joint. Naghibi et al. [20] studied the effect of tool offset on UTS of AISI 304 and AA5052 dissimilar FSW joint. Based on the results, the maximum of UTS occurs at 2 mm of offset. Kar et al. [21] investigated the tool offset effect on materials flow in FSW of Aluminum and Titanium and found that by increasing the tool offset, materials flow increases. Tamjidi et al. [22], by studying the effect of traveling speed, rotational speed, and tool offset, optimized the FSW process of AA6061 and AA7075 aluminum alloys. They found that by offsetting toward AA7075, the mechanical properties are improved. Safeen et al. [23] investigated the effect of parameters on FSW of AA6061-T6 statistically. They found that pin shape, rotational speed, travelling speed, and tilt angle have the most effects on UTS and hardness of joint, respectively. Periyasami et al. [24] also studied the effect of parameters on FSW of AA6061 and AA7075-T651 aluminum alloys. Based on the results, it was observed that the pin diameter, tool offset, and tilt angle have the most effects on UTS of joint, respectively. Derazkola et al. [25] investigated the effect of rotational speed, travel speed, plunge depth, and tilt angle on UTS of dissimilar FSW of AA5754 and Polymethyl methacrylate (PMMA) and found the optimum values of the mentioned parameters. The mentioned papers used single-factor tests, which means keeping one variable and keeping the other constant. Due to the high costs of experimental tests and much time consumption, researchers decided to use artificial intelligence (AI) to decrease the risks of joint production with voids and wasting money. For this reason, they used different approaches in relation to AI [26]. At the first step, the optimization of FSW process parameters is used for similar joints and, meanwhile, used for dissimilar joints. Joints considered are different aluminum alloy joints widely used in automobile industries. Table 1 presents the primary aluminum dissimilar joints optimized by AI techniques. Due to available literature, the main FSW factors considered are tool rotational and traverse velocities [27]. These parameters are the main factors to produce heat during the FSW process. Other factors such as tool pin size, tool shoulder size, tool tilt angle, and tool plunge depth are also considered. On the other hand, the CCD and ANOVA are commonly used to optimize FSW process parameters [28]. It can be concluded that all research outputs found the highest ultimate tensile strength after FSW of dissimilar aluminum joints.

Table 1. Summary of optimization of FSW process parameters at various dissimilar aluminum joints.

Aluminum Alloy Joint	Optimization Technique	FSW Parameter	Output	Reference
AA6351-T6 + AA6061-T6	Central composite rotatable design method	tool rotational speed, tool traverse speed and axial force	Ultimate tensile strength	[29]
AA6351-T6 + AA5083-H111	Response surface methodology	tool pin profile, tool rotational speed, welding speed, and axial force	Ultimate tensile strength	[30]
AA6082-T6 + AA5754-H111	Taguchi-based grey relational analysis	Tool shoulder diameter, pin diameter, tool rotational, and welding speeds	Ultimate tensile strength	[31]
AA5083-H111 + AA6082-T6	The central composite design (CCD) technique with response surface methodology (RSM)	Tool pin profile, tool rotational speed, welding speed, and axial force	Ultimate tensile strength	[32]
AA2024-T351 + AA7075-T651	Central composite rotatable design (CCRD)	Tool rotational speed, welding speed, and plunge depth	Ultimate tensile strength	[33]
AA2219-T87 + AA7075-T73	Taguchi mixed factorial design matrix	Tool rotational speed, welding speed, tool profile, and tilt angle	Ultimate tensile strength	[34]
AA6082-T6 + AA7050-T7	Grey-based Taguchi technique	Tool rotational speed and welding speed	Ultimate tensile strength	[35]

Based on the literature survey, three factors named tilt angle, plunge depth, and tool offset were investigated individually or combined with rotational speed, traveling speed, and tool geometry, in which this combination leads to a lack of understanding of these parameters' effectiveness. It should be noted that three mentioned factors are determinative of tool positioning in FSW process. Investigating the effect of these factors simultaneously with other parameters such as process speeds (rotational speed and translational speed) and tool geometry leads to a poor understanding of the impact of these factors on the FSW process. Because three mentioned parameters have same origin, they should be studied separately from other process parameters. Due to lack of investigation in this field, a deliberation seems to be necessary. Therefore, in this paper the effects of tilt angle, plunge depth, and tool offset on UTS of newly FSW joint between AA6061-T6 and AA7075-T6 have been investigated. In this manner, to design the experiments, optimization, and statistical analysis, Response Surface Methodology (RSM) has been used.

2. Materials and Methods

In the current study, AA6061-T6 and AA7075-T6 Aluminum alloys were used for performing FSW. The raw materials were provided from the local market (AmaLcast, Arak, Iran) and the properties of base metals were used from manufacturing company data sheets. Chemical composition and mechanical properties of mentioned alloys have been illustrated in Tables 2 and 3, respectively. The dimensions of workpieces were $100 \times 50 \times 5$ mm^3 and the welded surfaces were machined before welding and washed with Acetone to decrease the probability of aluminum oxide forming at weld nugget and consequently defect forming.

Table 2. Chemical composition of AA6061-T6 and AA7075-T6 Aluminum alloys [36].

Aluminum Alloy	Chemical Composition (%)								
AA6061-T6	Al Balance	Mg 0.81	Si 0.61	Cu 0.29	Fe 0.2	Cr 0.13	Mn 0.03	Zn 0.02	Ti 0.01
AA7075-T6	Al Balance	Zn 5.11	Mg 2.04	Cu 1.11	Fe 0.61	Si 0.33	Cr 0.229	Ti 0.027	Mn 0.014

Table 3. Mechanical properties of AA6061-T6 and AA7075-T6 Aluminum alloys [36].

Aluminum Alloy	Yield Stress (MPa)	UTS (MPa)	Elongation (%)
AA6061-T6	268	311	17
AA7075-T6	485	568	11

To perform friction stir welding, modified convectional milling machine (FU450R, Tabriz, Iran) was used (Figure 1a). Raw materials were fixed in steel-made fixtures during the FSW procedure. In accordance with the suggested procedure in the literature review, the harder alloy (AA7075-T6) was inset at retreating side to increase the joint strength and avoid defects forming [37]. It should be mentioned that in FSW of dissimilar materials, it is better to set the tool offset toward harder material where this instruction was performed in current study [38]. In this study, travelling speed and rotational speed were set at 90 mm/min and 1180 rpm for all experiments, respectively. A tool with a flat pin and shoulder was used to perform FSW for all experiments in which its shape and dimensions have been shown in Figure 1b. The tool is made of H13 work-hardened steel. After producing the tool, it was exposed to thermal hardening procedure based on related standards [3,39]. Dwelling time for all experiments were 5 s. All experiments (process parameters) were repeated three times and the average value was reported as the experimental test result.
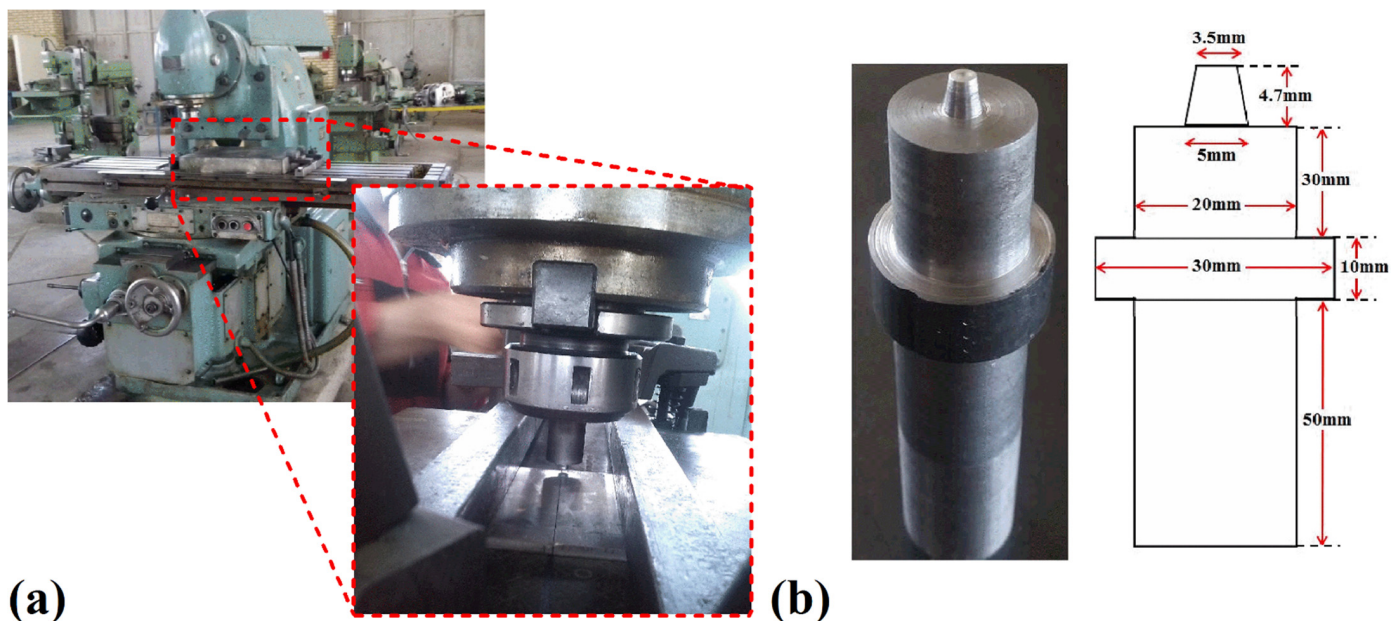
Figure 1. (**a**) FSW machine, (**b**) Tool used in FSW process.

To study the mechanical properties of friction stir welded specimens, standard tensile test was used. In this manner, three tensile test coupons for each specimen were prepared due to ASTM-E8 standard [40,41]. After performing the test by SANTAM-25KN apparatus (SANTAM, Tabriz, Iran) at 1 mm/min speed, the average of measured data was considered for each specimen. The schematic view and image of specimens and related tensile test coupons have been shown in Figure 2a,b, respectively.
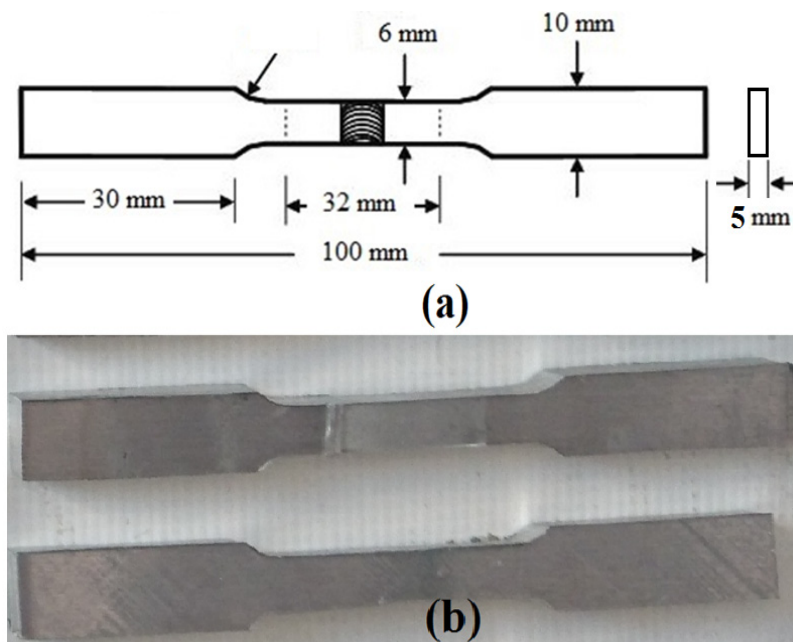
Figure 2. (**a**) The schematic view and (**b**) image of tensile test samples.

3. Design of Experiments

In this section, the design of experiments and important variables have been discussed. To study the main and interaction effects, Central Composite Design (CCD) has been utilized, and to implement this design, Analysis of Variance (ANOVA), Minitab (12, Minitab LLC, State College, PA, USA), and Design Expert software (12, Minitab LLC, State College, PA, USA) were performed.

In the current study, three variables named tilt angle, plunge depth, and tool offset have been considered as independent variables and UTS has been considered as a dependent variable. As discussed before, this FSW tool offset refers to shifting of tool axis from base metals interfaces (Figure 3a), and the tool tilt angle refers to the tilting of FSW tool axis from raw metals normal axis (Figure 3b). Based on CCD, every variable had five levels which have been illustrated in Table 4.
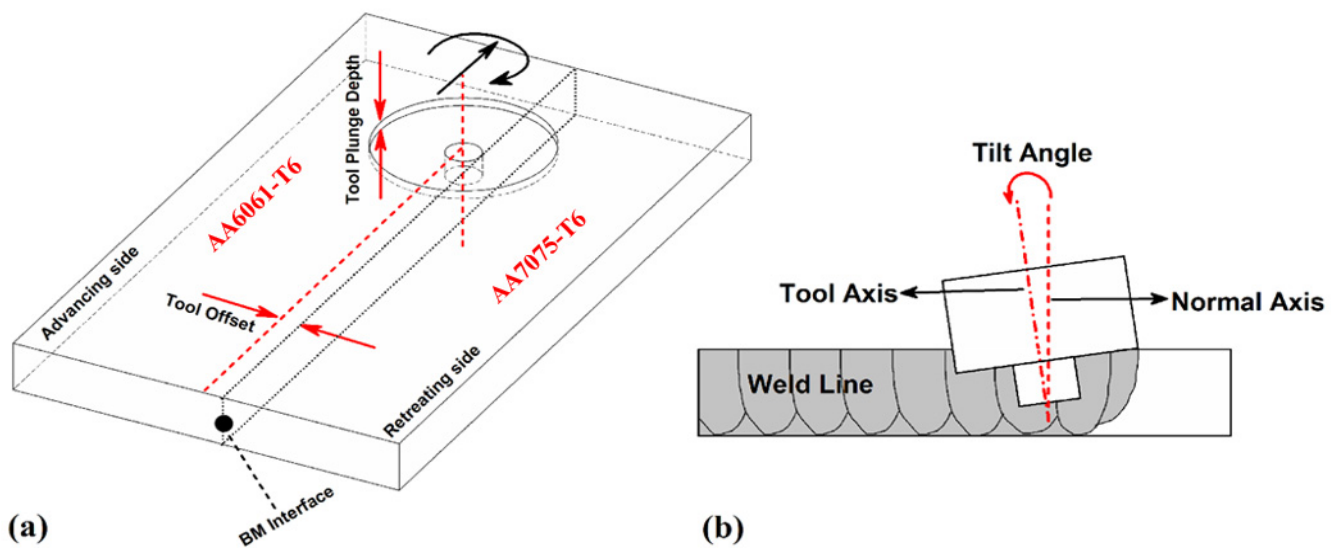

Figure 3. (**a**) Schematic view of tool offset and plunge depth, and (**b**) tool tilt angle.

Table 4. Considered variables and their level.

Factors	Unit	Level 1	Level 2	Level 3	Level 4	Level 5
Tool Offset	mm	0	0.5	1	1.5	2
Tilt Angle	Degree	0	1	2	3	4
Plunge Depth	mm	0	0.1	0.2	0.3	0.4

4. Results and Discussion

4.1. Model Deliberation and Variables Effectiveness

CCD was used to develop the design matrix. In this manner, twenty specimens were prepared and welded and their relative UTS values were measured. Design matrix and measured UTS have been illustrated in Table 5.

Table 5. Design matrix and UTS values.

Run	Tilt Angle (Degree)	Plunge Depth (mm)	Tool Offset (mm)	UTS (MPa)
1	1	0.1	0.5	265
2	1	0.1	1.5	230
3	3	0.1	0.5	278
4	3	0.1	1.5	244
5	1	0.3	0.5	241
6	1	0.3	1.5	204
7	3	0.3	0.5	233
8	3	0.3	1.5	215
9	2	0.2	0	244
10	2	0.2	2	196
11	0	0.2	1	235
12	4	0.2	1	260
13	2	0	1	265
14	2	0.4	1	185
15	2	0.2	1	262
16	2	0.2	1	265
17	2	0.2	1	268
18	2	0.2	1	265
19	2	0.2	1	266
20	2	0.2	1	272

In statistical studies, the R-Squared and Adjusted R-Squared values determine the accuracy of obtained regression equation. The coefficients of the statistical model have been illustrated in Table 6. In statistical analysis, 95% of confidence level was considered and ANOVA was used to study the main and interaction effects of variables. ANOVA test for UTS has been shown in Table 7.

Table 6. The statistical magnitude of regression model.

Source	Std. Dev.	R^2	Adjusted R^2	Predicted R^2	Press	
Linear	18.54	0.6061	0.5322	0.4008	8370.62	
2FI	20.30	0.6166	0.4396	0.2786	10,077.16	
Quadratic	5.07	0.9816	0.9651	0.8788	1692.37	Suggested
Cubic	3.20	0.9956	0.9861	0.9353	904.23	Aliased

To test the statistical model, normalization of statistical distribution of residuals and lack of self-correlation and independency among residuals are needed. Due to Table 6, quadratic regression model was chosen. The main factors, square, and interaction items constitute the ANOVA form or test. To evaluate the model, one must test it statistically, in which its results have been shown in Figure 4. Figure 4a,c are representative of scattering of residuals around the normal line. Thus, the model residuals have the normal distribution

process pattern. This result can be obtained by the Kolmogorov–Smirnov test. Figure 4b,d shows normal and independent distribution of residuals and lack of self-correlation among residuals, respectively.

Table 7. ANOVA test for UTS.

| Source	Sum of Squares	Degree of Freedom	Mean Square	F-Value	*p*-Value	
Model	13,711.71	9	1523.52	59.32	<0.0001	Significant
A-Tool Offset	3025.00	1	3025.00	117.78	<0.0001	Significant
B-Tilt Angle	400.00	1	400.00	15.57	0.0027	Significant
C-Plunge Depth	5041.00	1	5041.00	196.27	<0.0001	Significant
AB	50.00	1	50.00	1.95	0.1932	Not significant
AC	24.50	1	24.50	0.9539	0.3518	Not significant
BC	72.00	1	72.00	2.80	0.1250	Not significant
A^2	3424.44	1	3424.44	133.33	<0.0001	Significant
B^2	578.19	1	578.19	22.51	0.0008	Significant
C^2	2730.16	1	2730.16	106.30	<0.0001	Significant
Residual	256.84	10	25.68			
Lack of Fit	199.51	5	39.90	3.48	0.0987	Significant
Pure Error	57.33	5	11.47			
Cor Total	13,968.55	19				
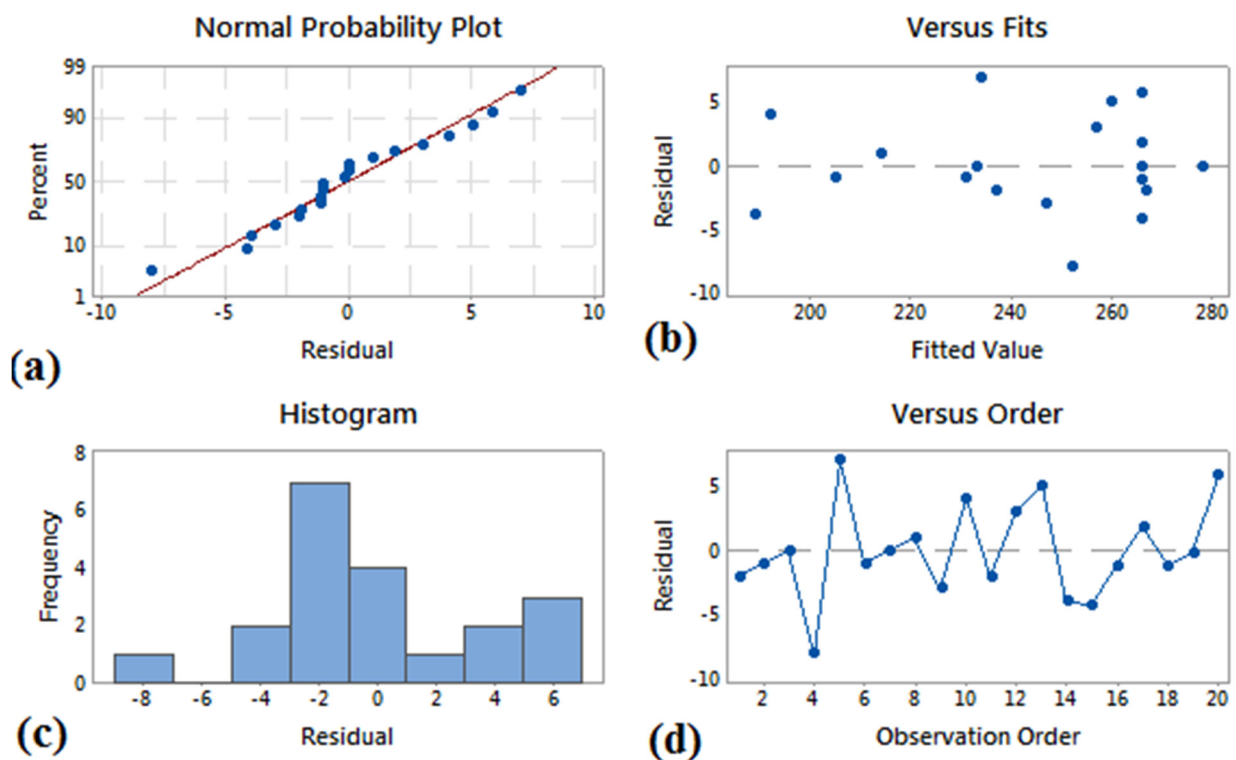
Figure 4. Evaluation results of statistical model (**a**) Residual-percent, (**b**) fitted value-residual, (**c**) residual-frequency, and (**d**) observation order-residual.

Through regression, UTS model was obtained as Equation (1):

$$UTS = 216.6 + 48.9A + 25.18B + 264.3C - 46.68A^2 - 4.80B^2 - 1042C^2 \qquad (1)$$

where A, B, and C are tool offset, tilt angle, and plunge depth, respectively. Due to ANOVA and Equation (1), the main factors affect the UTS directly. In Figure 5, the effectiveness of factors has been illustrated as normal plot and Pareto chart. The Pareto chart highlights

the most important among a set of factors. Based on Figure 5, the most important factor among a set of factors on UTS are plunge depth, tool offset, and tilt angle, respectively.
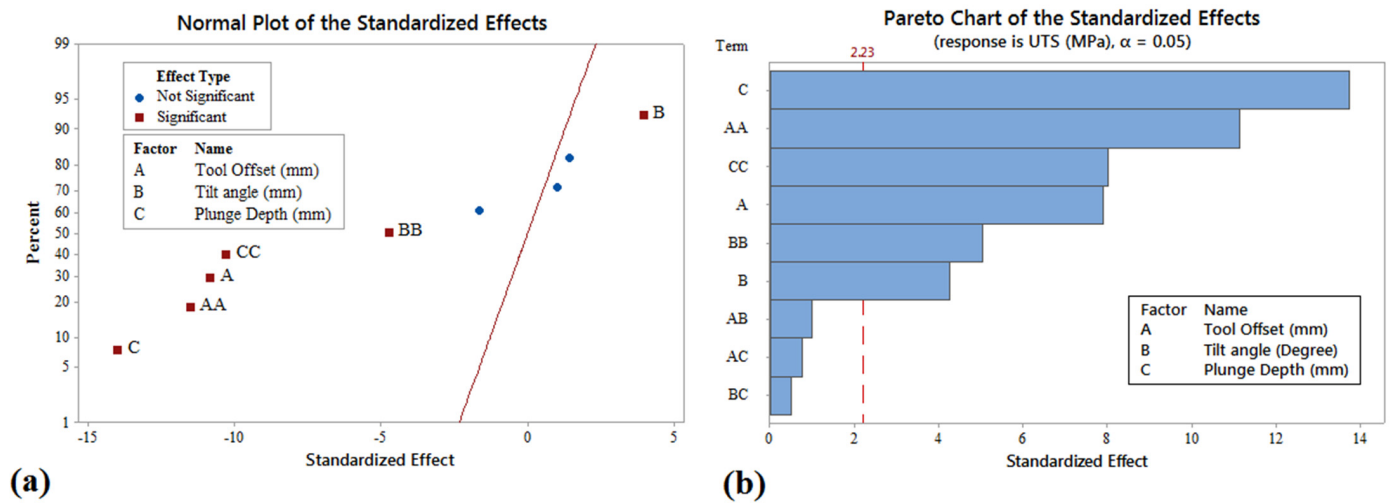

Figure 5. The effectiveness of model factors (**a**) Normal plot (**b**) Pareto plot.

4.2. Tool Offsetting

In general, in the FSW of dissimilar materials, the portion of participation of materials determines the joint properties [42,43]. Imbalance in the volume ratio of plastic flow leads to inappropriate material mixing at weld nugget and finally increment in defects density [44–46]. The tool offset in the dissimilar joint is an essential issue because it increases FSW tool life and base metal mixing. It is proved that the FSW tool offsets in the harder metal side have crucial effects to improve the final joint quality in a dissimilar joint [47]. In this regard, the FSW tool is offset in AA7075 aluminum alloy in this study. The tensile strength of AA7075 is more than the AA6061 aluminum alloy. The proper volume ratio of materials depends on different materials' mechanical properties and, generally, the plastic flow portion of material with greater UTS. As mentioned before, this factor is unique for every pair of dissimilar materials. In Figure 6, the UTS vs. tool offset for welded specimens have been shown. According to the results, the tool offset from 0 mm until 0.7 mm increased as the tensile strength of the joint increased. With the increasing tool offset of more than 0.7 mm, the interaction at the interface of base metals decreased. Due to rising tool offset inside the AA7075 aluminum alloy, the FSW pin tool stirring action decreased in the AA6061 alloy side, and for this reason, the tensile strength of the final joint that welded more than 0.7 mm tool offset was decreased.

Based on the obtained results, it is clear that tool offsetting leads to significant increments in joint efficiency. The mean UTS had an increasing trend until 0.7 mm on the AA7075-T6 side, and after that, the UTS of the joint decreased. In addition, due to obtained results and statistical analysis, it was shown that the maximum joint efficiency could be achieved at 0.7 mm of offset toward AA7075-T6. The results show that the maximum tensile strength in 0.7 mm tool offset was ~270 MPa, and the minimum tensile strength obtained at 2 mm tool offset was ~185 MPa.

4.3. Tool Tilt Angle

The presence of tilt angle causes the plasticized materials under the tool shoulder while tool traveling comes back to weld nugget by forging force [48]. The forging force condenses plasticized metals in the stir zone by intense pressure and forms the joint area. It should be noted that the tilt angle has an optimum value. By receding from the optimum point, the contact area between tool shoulder and workpiece decreases, which leads to decrement in heat and vertical plastic flow generated by tool shoulder, and consequently, mechanical metallurgical properties drop. Proper compression and interference occur

by forging the plastic flow in tool tilt angle, leading to decrement in volume defects like porosity at weld nugget. On the other hand, using a proper tilt angle causes an increment in UTS and the development of a homogenous and uniform microstructure at the weld nugget. The results from UTS vs. tilt angle plot are shown in Figure 7.
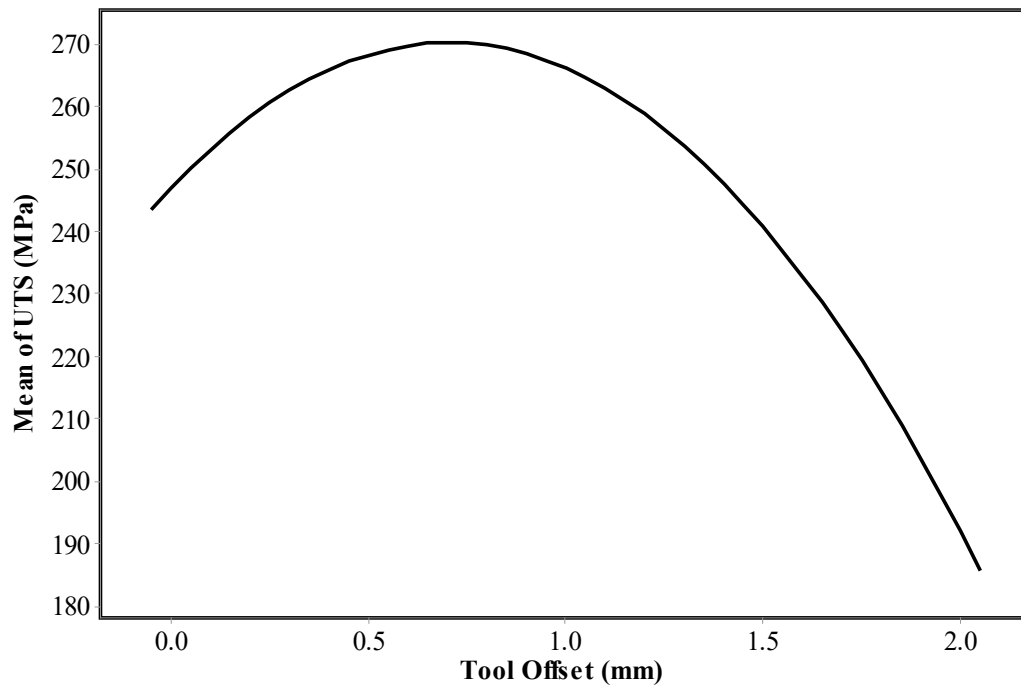

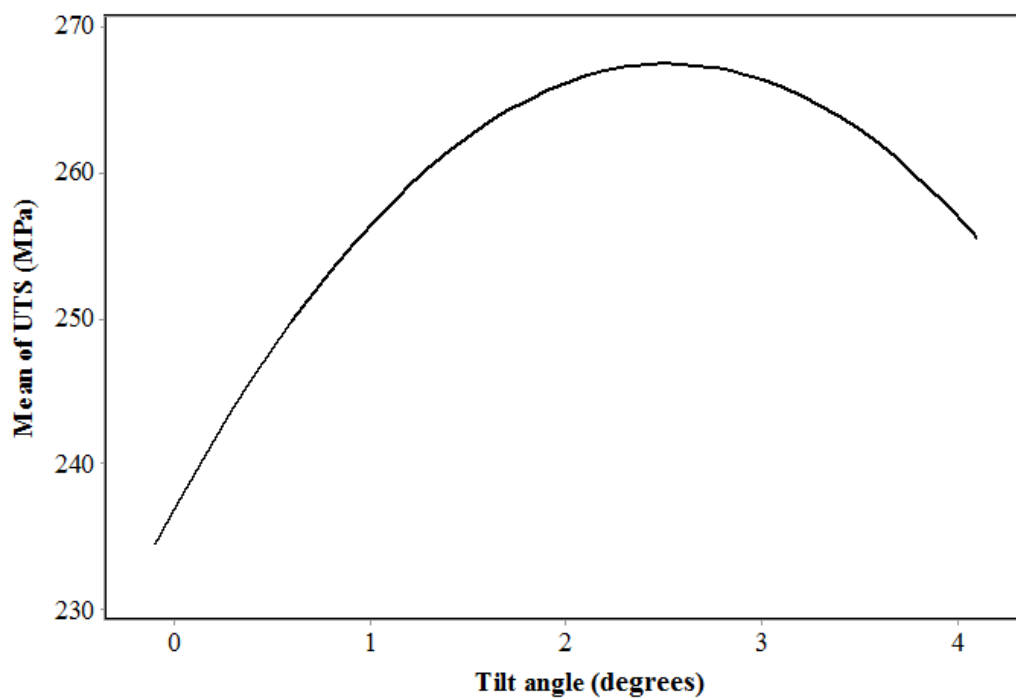**Figure 6.** UTS vs. tool offset for welded specimens.

Figure 7. UTS vs. tool tilt angle for welded specimens.

Due to selected tilt angle range in this study (0–4°), the UTS of final joint had an increasing trend from 0° until 2.6°, and after that decreased. The obtained results revealed

that the lowest tensile strength joint was formed by 0° tool tilt angle and the highest tensile strength joint was formed by 2.6° tool tilt angle.

The least UTS occurs at specimen with low tilt angle. One of the common defects that happens in inappropriate tilt angle is the lack of fill defect. In the case of zero or inappropriate tilt angle, because of inopportune forging, longitudinal slits with various depths are composed at tool tilt.

The surfaces of friction stir welded specimens with various tilt angles have been shown in Figure 8. Based on the results, specimens with zero and one degrees of tilt angle exhibit a lack of fill defects. It is approved that the forging force is not enough at a low tool tilt angle to fill the joint line [39]. For this reason, the lack of filling of the joint line at the surface can be seen. By increasing the tilt angle, the length of longitudinal slits decreases and at two degrees of tilt angle, the surface defect disappears completely. At a high tool tilt angle, the tool prevents material's extrusion from advancing side into retreating side. For this reason, the plasticized material condensed in the vicinity of the joint line and formed a surface flash. On the other hand, at a higher tool tilt angle, surface flash forms in the vicinity of the joint line. The obtained results indicate that the surface flash formed from a 3° tilt angle and increased at a 4° tool tilt angle. The surface defects (lack of filling) and side flash are the main reasons that decrease the strength of welded samples.
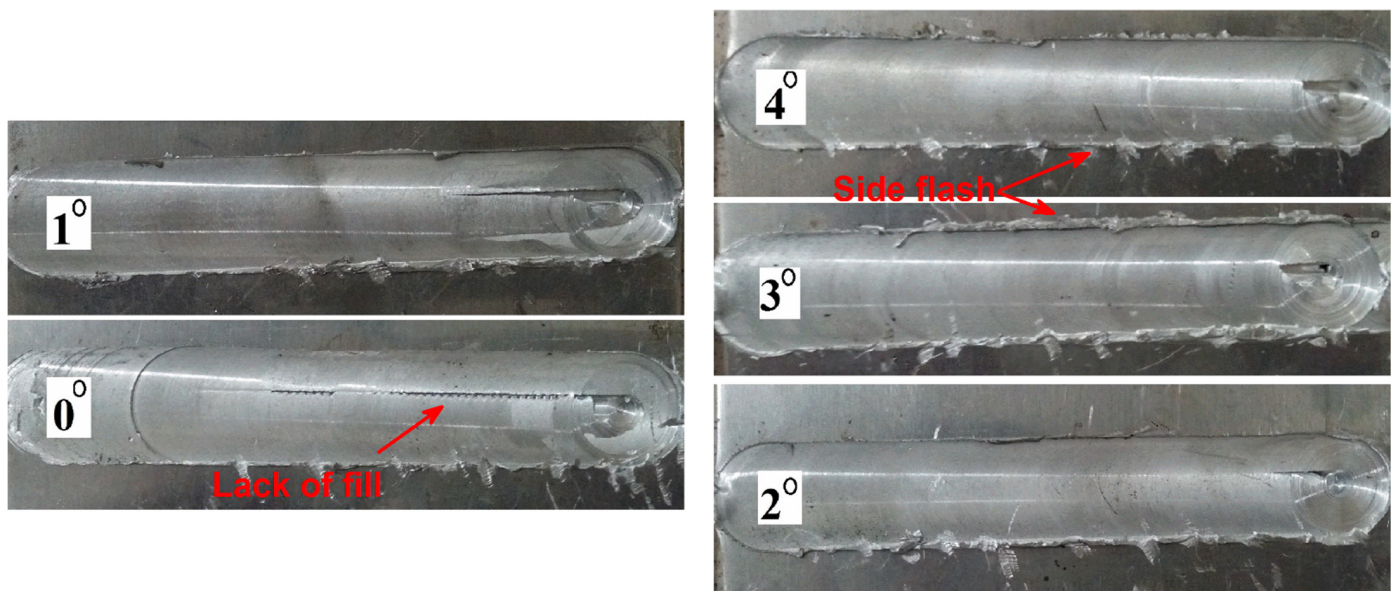

Figure 8. Welded specimens with various tilt angles.

4.4. Tool Plunge Depth

The area beneath the workpiece experiences the least heat because of being locating at a further distance from the tool shoulder, and a little thermal softening and hard plastic flow take place [49].

The possibility formation of weld root defects, like tunneling in the lower area of the joint line and beneath of workpieces, is high [50,51]. To remove root defects in the FSW joint line, controlling plunge depth is very important. FSW tool plunge depth can increase the stirring action of materials in the stir zone and control heat input in the joint line. Using proper plunge depth leads to better plastic flow and increased heat transfer to bottom of pin [3,9,39]. By penetration of tool shoulder in specimen, friction interaction between specimen and tool increases extremely and causes significant increment in heat generation and vertical plastic flow. Forming a proper vertical plastic flow leads to the improvement of the microstructure and mechanical properties. In Figure 9a, UTS vs. plunge depth plot for welded specimens has been illustrated. Based on Figure 9, using the optimum value of plunge depth can cause increment in UTS of joint. In the current study, a tool with

4.6 mm of length and workpiece with 5 mm of thickness was used. Had plunge depth not been used, a thickness of 0.4 mm of bottom of specimen would have been without any significant stirring and could have been like a support for deformed materials. Using plunge depth can lead to better plastic flow at bottom of specimen and decrement in support area. By applying large plunge depths, plastic flow concentration at weld nugget misses and material ejection from the bottom of specimen takes place, which leads to extreme decrement in metallurgical and mechanical properties. In Figure 9b, the bottom view of specimens with various plunge depths have been shown. As seen, at 0 mm of plunge depth, the bottom slit has not been connected, while at 1 mm of plunge depth, the situation of bottom slit is different and complete connection can be seen. In addition, material ejection is not observed. By increasing the plunge depth, material ejection takes place, based on Figure 9a, and UTS decreases intensely.
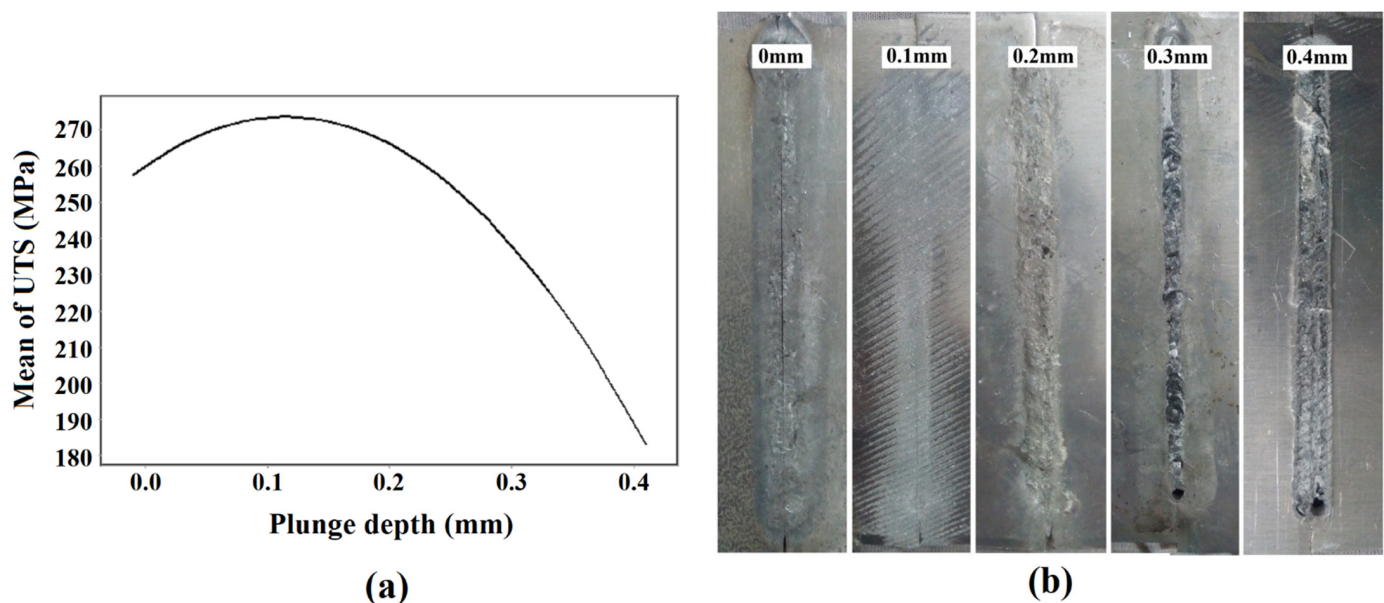

Figure 9. (**a**) UTS vs. plunge depth, and (**b**) welded specimens with various plunge depths.

4.5. Optimization

In Figure 10a–c, three-dimensional plots and contour plots of variables affecting UTS have been illustrated. Based on obtained results, all variables (plunge depth, tool offset, and tilt angle) and their interaction had significant effects on UTS of joint. In Figure 10d, the optimum values of mentioned variables and maximum UTS have been illustrated. Due to statistically obtained results, 0.7 mm of tool offset, 2.7 degrees of tilt angle, and 0.1 mm of plunge depth were the optimum values which lead to 281 MPa of UTS and 90% of joint efficiency. This situation could be used to determine the tool positioning.

To validate the model output, a specific specimen was friction stir welded with optimum parameters proposed by the model. For production of this joint, the FSW tool offset, plunge depth, and tilt angle selected 0.7 mm, 0.1 mm, and 2.6°, respectively. Figure 11 presented the surface flow and bottom of the FSWed joint with optimum parameters. The UTS of the FSWed sample was measured and compared with the optimization result. A comparison between predicted and measured UTS has been done in Table 8. The results revealed that the predicted UTS was 272 MPa, and the FSWed sample UTS was 281 MPa. The predicted model and experimental results were ~3% (near 9 MPa). This result shows good agreements of predicted model and experimental data.
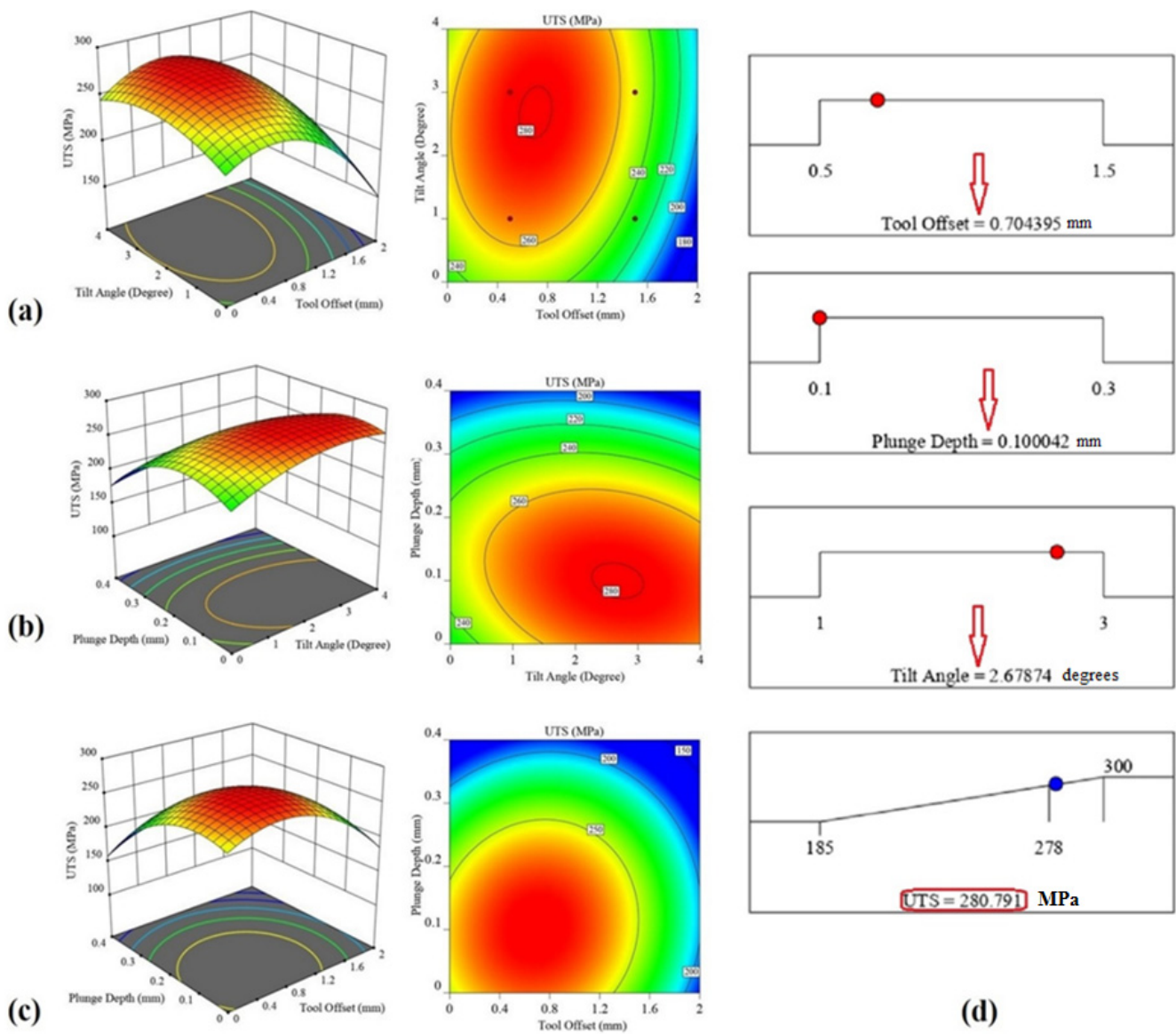
Figure 10. Three dimensional and contour plots of (**a**) tool offset and tilt angle effects on UTS, (**b**) plunge depth and tilt angle effects on UTS, (**c**) plunge depth and tool offset effects on UTS, (**d**) optimum values of main variables.
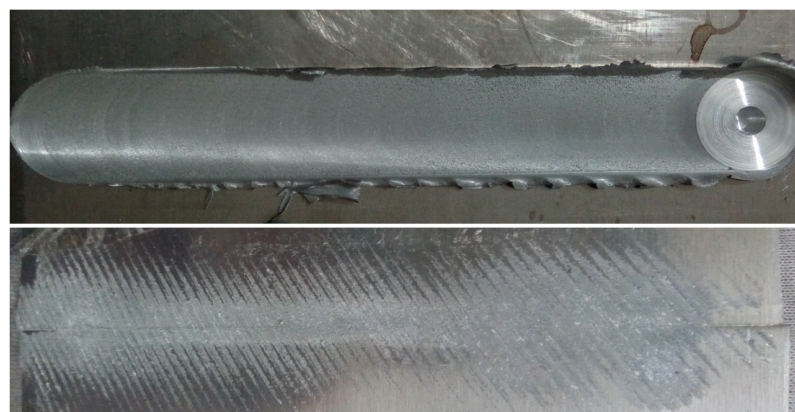

Figure 11. The top and bottom views of welded specimen due to optimum situations.

Table 8. The statistical and experimental UTS magnitudes of optimized model.

Tool Offset (mm)	Tilt Angle (Degrees)	Plunge Depth (mm)	UTS (MPa) Predicted	UTS (MPa) Experimental
0.7	2.7	1	272	281

5. Conclusions

In this paper, the effects of plunge depth, tool offset, and tilt angle on UTS of FSW joint of AA6061-T6 and AA7075-T6 were investigated experimentally and statistically. RSM was used for designing the experiments, optimization, and analysing the results. The following outcomes were obtained:

1. Experimental tests were carried out to find the maximum achievable UTS of joint. Based on optimization procedure, the optimum values were determined as 0.7 mm of tool offset, 2.7 degrees of tilt angle, and 0.1 mm of plunge depth. These values resulted in a UTS of 281 MPa. In comparison to UTS of base metals, the joint efficacy of FSW sample was near 90 percent.
2. The low tool plunge depth and tilt angle can form a lack of filling in the surface of the joint, and on the other hand, the high value of tool plunge depth and tilt angle caused the surface flash. Both types of defects decrease the properties of the final joint.
3. In the welded cases with no plunge depth, the connection of specimens at the bottom were not properly performed, while at 1 mm of the plunge depth, two specimens were connected completely and by exceeding the plunge depth, material ejection from the bottom of specimens took place.
4. In the case of using small tilt angle, longitudinal slits with various depths were formed at tool tail and the lack of filling-in defect was observed. By increasing the tilt angle to 2 degrees, mentioned defects vanished completely. The FSW tool offset from 0 until 0.1 mm shows a slight increase, and after that, from 0.1 until 0.4 mm, the UTS decreased. The obtained results indicated that the sensitivity of FSW tool offset on UTS is more than FSW tool plunge depth and FSW tool tilt angle in this joint.

Author Contributions: Conceptualization, A.G., S.M.N., W.S., J.T., S.M. and H.A.D.; methodology, A.G., S.M.N. and S.M.; software, A.G., S.M.N., W.S. and S.M.; validation, A.G., S.M.N., W.S., S.M. and H.A.D.; formal analysis, A.G., S.M.N., W.S., J.T., S.M. and H.A.D.; investigation, A.G., S.M.N., W.S. and H.A.D.; resources, A.G., S.M.N., W.S. and S.M.; data curation, A.G.; writing—original draft preparation, A.G., J.T., S.M. and H.A.D.; writing—review and editing, A.G., S.M.N., W.S., J.T., S.M. and H.A.D.; visualization, A.G. and H.A.D.; supervision, A.G.; project administration, A.G.; funding acquisition, A.G. All authors have read and agreed to the published version of the manuscript.

Institutional Review Board Statement: Not applicable.

Informed Consent Statement: Not applicable.

Data Availability Statement: Not applicable.

Conflicts of Interest: The authors declare no conflict of interest.

References

1. Aghajani Derazkola, H.; Khodabakhshi, F. Intermetallic compounds (IMCs) formation during dissimilar friction-stir welding of AA5005 aluminum alloy to St-52 steel: Numerical modeling and experimental study. *Int. J. Adv. Manuf. Technol.* **2019**, *100*, 2401–2422. [CrossRef]
2. Elyasi, M.; Derazkola, H.A. Experimental and thermomechanical study on FSW of PMMA polymer T-joint. *Int. J. Adv. Manuf. Technol.* **2018**, *97*, 1445–1456. [CrossRef]
3. Aghajani Derazkola, H.; Eyvazian, A.; Simchi, A. Submerged friction stir welding of dissimilar joints between an Al-Mg alloy and low carbon steel: Thermo-mechanical modeling, microstructural features, and mechanical properties. *J. Manuf. Process.* **2020**, *50*, 68–79. [CrossRef]

4. Ghiasvand, A.; Yavari, M.M.; Tomków, J.; Grimaldo Guerrero, J.W.; Kheradmandan, H.; Dorofeev, A.; Memon, S.; Derazkola, H.A. Investigation of Mechanical and Microstructural Properties of Welded Specimens of AA6061-T6 Alloy with Friction Stir Welding and Parallel-Friction Stir Welding Methods. *Materials* **2021**, *14*, 6003. [CrossRef]

5. Akbari, M.; Aliha, M.R.M.; Keshavarz, S.M.E.; Bonyadi, A. Effect of tool parameters on mechanical properties, temperature, and force generation during FSW. *Proc. Inst. Mech. Eng. Part L J. Mater. Des. Appl.* **2016**, *233*, 1033–1043. [CrossRef]

6. Patel, V.; Li, W.; Vairis, A.; Badheka, V. Recent Development in Friction Stir Processing as a Solid-State Grain Refinement Technique: Microstructural Evolution and Property Enhancement. *Crit. Rev. Solid State Mater. Sci.* **2019**, *44*, 378–426. [CrossRef]

7. Derazkola, H.A.; Elyasi, M.; Hamed Aghajani Derazkola, M.E. The influence of process parameters in friction stir welding of Al-Mg alloy and polycarbonate. *J. Manuf. Process.* **2018**, *35*, 88–98. [CrossRef]

8. Derazkola, H.A.; Eyvazian, A.; Simchi, A. Modeling and experimental validation of material flow during FSW of polycarbonate. *Mater. Today Commun.* **2020**, *22*, 100796. [CrossRef]

9. Eyvazian, A.; Hamouda, A.M.A.M.; Aghajani Derazkola, H.; Elyasi, M. Study on the effects of tool tile angle, offset and plunge depth on friction stir welding of poly(methyl methacrylate) T-joint. *Proc. Inst. Mech. Eng. Part B J. Eng. Manuf.* **2019**, *234*, 773–787. [CrossRef]

10. Memon, S.; Tomków, J.; Derazkola, H.A. Thermo-Mechanical Simulation of Underwater Friction Stir Welding of Low Carbon Steel. *Materials* **2021**, *14*, 4953. [CrossRef] [PubMed]

11. Aghajani Derazkola, H.; Khodabakhshi, F.; Gerlich, A.P. Friction-forging tubular additive manufacturing (FFTAM): A new route of solid-state layer-upon-layer metal deposition. *J. Mater. Res. Technol.* **2020**, *9*, 15273–15285. [CrossRef]

12. Aghajani Derazkola, H.; Simchi, A. A new procedure for the fabrication of dissimilar joints through injection of colloidal nanoparticles during friction stir processing: Proof concept for AA6062/PMMA joints. *J. Manuf. Process.* **2020**, *49*, 335–343. [CrossRef]

13. Aghajani Derazkola, H.; Simchi, A.; Hamed Aghajani Derazkola, A.S. Experimental and thermomechanical analysis of the effect of tool pin profile on the friction stir welding of poly(methyl methacrylate) sheets. *J. Manuf. Process.* **2018**, *34*, 412–423. [CrossRef]

14. Qin, D.Q.; Fu, L.; Shen, Z.K. Visualisation and numerical simulation of material flow behaviour during high-speed FSW process of 2024 aluminium alloy thin plate. *Int. J. Adv. Manuf. Technol.* **2019**, *102*, 1901–1912. [CrossRef]

15. Zhai, M.; Wu, C.; Shi, L. Tool tilt angle induced variation of shoulder-workpiece contact condition in friction stir welding. *Sci. Technol. Weld. Join.* **2022**, *27*, 68–76. [CrossRef]

16. Kumar, S.S.; Murugan, N.; Ramachandran, K.K. Effect of tool tilt angle on weld joint properties of friction stir welded AISI 316L stainless steel sheets. *Measurement* **2020**, *150*, 107083. [CrossRef]

17. Rajendran, C.; Srinivasan, K.; Balasubramanian, V.; Balaji, H.; Selvaraj, P. Effect of tool tilt angle on strength and microstructural characteristics of friction stir welded lap joints of AA2014-T6 aluminum alloy. *Trans. Nonferrous Met. Soc. China* **2019**, *29*, 1824–1835. [CrossRef]

18. Zheng, Q.; Feng, X.; Shen, Y.; Huang, G.; Zhao, P. Effect of plunge depth on microstructure and mechanical properties of FSW lap joint between aluminum alloy and nickel-base alloy. *J. Alloys Compd.* **2017**, *695*, 952–961. [CrossRef]

19. Ramachandran, K.K.; Murugan, N.; Shashi Kumar, S. Effect of tool axis offset and geometry of tool pin profile on the characteristics of friction stir welded dissimilar joints of aluminum alloy AA5052 and HSLA steel. *Mater. Sci. Eng. A* **2015**, *639*, 219–233. [CrossRef]

20. Darzi Naghibi, H.; Shakeri, M.; Hosseinzadeh, M. Neural Network and Genetic Algorithm Based Modeling and Optimization of Tensile Properties in FSW of AA 5052 to AISI 304 Dissimilar Joints. *Trans. Indian Inst. Met.* **2016**, *69*, 891–900. [CrossRef]

21. Kar, A.; Suwas, S.; Kailas, S.V. Significance of tool offset and copper interlayer during friction stir welding of aluminum to titanium. *Int. J. Adv. Manuf. Technol.* **2019**, *100*, 435–443. [CrossRef]

22. Tamjidy, M.; Baharudin, B.T.H.T.; Paslar, S.; Matori, K.A.; Sulaiman, S.; Fadaeifard, F. Multi-Objective Optimization of Friction Stir Welding Process Parameters of AA6061-T6 and AA7075-T6 Using a Biogeography Based Optimization Algorithm. *Materials* **2017**, *10*, 533. [CrossRef] [PubMed]

23. Safeen, W.; Hussain, S.; Wasim, A.; Jahanzaib, M.; Aziz, H.; Abdalla, H. Predicting the tensile strength, impact toughness, and hardness of friction stir-welded AA6061-T6 using response surface methodology. *Int. J. Adv. Manuf. Technol.* **2016**, *87*, 1765–1781. [CrossRef]

24. Kunnathur Periyasamy, Y.; Perumal, A.V.; Kunnathur Periyasamy, B. Optimization of process parameters on friction stir welding of AA7075-T651 and AA6061 joint using response surface methodology. *Mater. Res. Express* **2019**, *6*, 96558. [CrossRef]

25. Derazkola, H.A.; Simchi, A. An investigation on the dissimilar friction stir welding of T-joints between AA5754 aluminum alloy and poly(methyl methacrylate). *Thin-Walled Struct.* **2019**, *135*, 376–384. [CrossRef]

26. Kumar, R.; Singh Dhami, S.; Mishra, R.S. Optimization of friction stir welding process parameters during joining of aluminum alloys of AA6061 and AA6082. *Mater. Today Proc.* **2021**, *45*, 5368–5376. [CrossRef]

27. Nait Salah, A.; Mehdi, H.; Mehmood, A.; Wahab Hashmi, A.; Malla, C.; Kumar, R. Optimization of process parameters of friction stir welded joints of dissimilar aluminum alloys AA3003 and AA6061 by RSM. *Mater. Today Proc.* **2021**. [CrossRef]

28. Haribalaji, V.; Boopathi, S.; Mohammed Asif, M. Optimization of friction stir welding process to join dissimilar AA2014 and AA7075 aluminum alloys. *Mater. Today Proc.* **2022**, *50*, 2227–2234. [CrossRef]

29. Prasanth, R.S.S.; Hans Raj, K. Determination of Optimal Process Parameters of Friction Stir Welding to Join Dissimilar Aluminum Alloys Using Artificial Bee Colony Algorithm. *Trans. Indian Inst. Met.* **2018**, *71*, 453–462. [CrossRef]

30. Palanivel, R.; Koshy Mathews, P.; Murugan, N. Optimization of process parameters to maximize ultimate tensile strength of friction stir welded dissimilar aluminum alloys using response surface methodology. *J. Cent. South Univ.* **2013**, *20*, 2929–2938. [CrossRef]
31. Kasman, Ş. Multi-response optimization using the Taguchi-based grey relational analysis: A case study for dissimilar friction stir butt welding of AA6082-T6/AA5754-H111. *Int. J. Adv. Manuf. Technol.* **2013**, *68*, 795–804. [CrossRef]
32. Anil Kumar, H.M.; Venkata Raman, V.; Shanmughanathan, S.P.; John, J.; Mohammed Iqbal, U. *Optimization of Dissimilar Friction Stir Welding Process Parameters of AA5083-H111 and AA6082-T6 by CCD-RSM Technique BT—Advances in Manufacturing Processes*; Vijay Sekar, K.S., Gupta, M., Arockiarajan, A., Eds.; Springer: Singapore, 2019; pp. 49–60.
33. Zhang, C.; Huang, G.; Cao, Y.; Wu, X.; Huang, X.; Liu, Q. Optimization of Tensile and Corrosion Properties of Dissimilar Friction Stir Welded AA2024-7075 Joints. *J. Mater. Eng. Perform.* **2019**, *28*, 183–199. [CrossRef]
34. Dinesh Kumar, R.; Ilhar Ul Hassan, M.S.; Muthukumaran, S.; Venkateswaran, T.; Sivakumar, D. Single and Multi-Response Optimization and Validation of Mechanical Properties in Dissimilar Friction Stir Welded AA2219-T87 and AA7075-T73 Alloys Using T-GRA. *Exp. Tech.* **2019**, *43*, 245–259. [CrossRef]
35. Singh, A.; Upadhyay, V. A Study on Optimization of Welding Parameters and their Effect on Joint Properties of Dissimilar AA6082-T6 and AA7050-T7 Friction Stir Welds. *J. Inst. Eng. Ser. D* **2021**, *102*, 249–269. [CrossRef]
36. Available online: https://www.iralco.ir/ (accessed on 1 January 2022).
37. Raturi, M.; Garg, A.; Bhattacharya, A. Joint strength and failure studies of dissimilar AA6061-AA7075 friction stir welds: Effects of tool pin, process parameters and preheating. *Eng. Fail. Anal.* **2019**, *96*, 570–588. [CrossRef]
38. Ahmad Shah, L.H.; Sonbolestan, S.; Midawi, A.R.H.; Walbridge, S.; Gerlich, A. Dissimilar friction stir welding of thick plate AA5052-AA6061 aluminum alloys: Effects of material positioning and tool eccentricity. *Int. J. Adv. Manuf. Technol.* **2019**, *105*, 889–904. [CrossRef]
39. Elyasi, M.; Derazkola, H.A.; Hosseinzadeh, M. Investigations of tool tilt angle on properties friction stir welding of A441 AISI to AA1100 aluminium. *Proc. Inst. Mech. Eng. Part B J. Eng. Manuf.* **2016**, *230*, 1234–1241. [CrossRef]
40. Derazkola, H.A.; Khodabakhshi, F.; Gerlich, A.P. Fabrication of a nanostructured high strength steel tube by friction-forging tubular additive manufacturing (FFTAM) technology. *J. Manuf. Process.* **2020**, *58*, 724–735. [CrossRef]
41. Derazkola, H.A.; Khodabakhshi, F. A novel fed friction-stir (FFS) technology for nanocomposite joining. *Sci. Technol. Weld. Join.* **2020**, *25*, 98–100. [CrossRef]
42. Aghajani Derazkola, H.; Kordani, N.; Aghajani Derazkola, H. Effects of friction stir welding tool tilt angle on properties of Al-Mg-Si alloy T-joint. *CIRP J. Manuf. Sci. Technol.* **2021**, *33*, 264–276. [CrossRef]
43. Derazkola, H.A.; MohammadiAbokheili, R.; Kordani, N.; Garcia, E.; Murillo-Marrodán, A. Evaluation of nanocomposite structure printed by solid-state additive manufacturing. *CIRP J. Manuf. Sci. Technol.* **2022**, *37*, 174–184. [CrossRef]
44. Khalaf, H.I.; Al-Sabur, R.; Abdullah, M.E.; Kubit, A.; Derazkola, H.A. Effects of Underwater Friction Stir Welding Heat Generation on Residual Stress of AA6068-T6 Aluminum Alloy. *Materials* **2022**, *15*, 2223. [CrossRef]
45. Aghajani Derazkola, H.; Garcia, E.; Elyasi, M. Underwater friction stir welding of PC: Experimental study and thermo-mechanical modelling. *J. Manuf. Process.* **2021**, *65*, 161–173. [CrossRef]
46. Bokov, D.O.; Jawad, M.A.; Suksatan, W.; Abdullah, M.E.; Świerczyńska, A.; Fydrych, D.; Derazkola, H.A. Effect of Pin Shape on Thermal History of Aluminum-Steel Friction Stir Welded Joint: Computational Fluid Dynamic Modeling and Validation. *Materials* **2021**, *14*, 7883. [CrossRef] [PubMed]
47. Shen, Z.; Ding, Y.; Gerlich, A.P. Advances in friction stir spot welding. *Crit. Rev. Solid State Mater. Sci.* **2020**, *45*, 457–534. [CrossRef]
48. Abd Elnabi, M.M.; Osman, T.A.; El Mokadem, A.; Elshalakany, A.B. Evaluation of the formation of intermetallic compounds at the intermixing lines and in the nugget of dissimilar steel/aluminum friction stir welds. *J. Mater. Res. Technol.* **2020**, *9*, 10209–10222. [CrossRef]
49. Memon, S.; Murillo-Marrodán, A.; Lankarani, H.M.; Aghajani Derazkola, H. Analysis of Friction Stir Welding Tool Offset on the Bonding and Properties of Al–Mg–Si Alloy T-Joints. *Materials* **2021**, *14*, 3604. [CrossRef] [PubMed]
50. Derazkola, H.A.; Aval, H.J.; Elyasi, M. Analysis of process parameters effects on dissimilar friction stir welding of AA1100 and A441 AISI steel. *Sci. Technol. Weld. Join.* **2015**, *20*, 553–562. [CrossRef]
51. Eyvazian, A.; Hamouda, A.; Tarlochan, F.; Derazkola, H.A.; Khodabakhshi, F. Simulation and experimental study of underwater dissimilar friction-stir welding between aluminium and steel. *J. Mater. Res. Technol.* **2020**, *9*, 3767–3781. [CrossRef]